

**Regular collision of dilatonic inflating branes**

Emily Leeper, Kazuya Koyama, and Roy Maartens

*Institute of Cosmology & Gravitation, University of Portsmouth, Portsmouth, PO1 2EG, United Kingdom*

(Received 30 August 2005; published 10 February 2006)

We demonstrate that a two-brane system with a bulk scalar field driving power-law inflation on the branes has an instability in the radion. We solve for the resulting trajectory of the brane, and find that the instability can lead to collision. Brane quantities such as the scale factor are shown to be regular at this collision. In addition we describe the system using a low-energy expansion. The low-energy expansion accurately reproduces the known exact solution, but also identifies an alternative solution for the bulk metric and brane trajectory.

DOI: [10.1103/PhysRevD.73.043506](https://doi.org/10.1103/PhysRevD.73.043506)

PACS numbers: 98.80.Cq, 04.50.+h

**I. INTRODUCTION**

In the search for a theory that can describe both quantum mechanics and gravity, string theory (which describes matter as vibrating strings moving in 11 dimensions) seems a strong candidate. It has been the subject of much research, and many different realizations of string theory have been found to be possible. This being so, experimental constraints on the theory are vital. It is hoped that the next generation of particle accelerators now being built will reach energies where some sign of extra dimensions may be seen, while laboratory gravity experiments at low energies can put constraints on the length scale of any extra dimensions. In cosmology, we can probe both the highest energies, through understanding of the early universe, and the largest scales available to us; thus an understanding of how string theory and extra dimensions affects cosmology is very valuable.

The fact that we observe only three spatial dimensions has to be explained away in string theory—this can be done by compactifying the extra dimensions to very small scales, or by attaching all the strings corresponding to normal matter to a four-dimensional surface called a brane. Five-dimensional models based on this latter method of dimensional reduction were presented in two papers by Randall and Sundrum in 1999 [1]. Much work has been done on cosmological generalizations of these models since then. Early universe inflation in braneworlds has been extensively studied, mostly driven by some kind of inflaton field, either localized on the brane with the other matter fields [2], or living in the whole bulk [3,4]. In this paper we will be considering a model of bulk-driven inflation.

In [5], Koyama and Takahashi found an exact solution for a five-dimensional bulk metric where a bulk scalar field with non-Bogomol'nyi-Prasad-Sommerfield (BPS) exponential potential drives power-law inflation on a single brane. This scenario is particularly attractive as the cosmological perturbations, normally an intractable problem in braneworld scenarios, can be solved exactly [6].

In [7], Mukohyama and Coley developed the scenario to include two branes. They found that for any value of the brane tension on the second brane there is one location where the second brane will remain at a constant bulk

coordinate away from the first brane. This is somewhat analogous to the scenario with two de Sitter (dS) branes and an empty Anti-de Sitter (AdS) bulk studied by Gen and Sasaki [8]. However unlike the static de Sitter model, the presence of the scalar field means that the constant coordinate separation does not lead to a static equilibrium as the proper distance between the two branes is time dependent.

The stability of this two-brane model against a wide class of metric perturbations was shown in [7]. Although it was shown that there were no unstable bulk metric perturbations, including perturbations of the bulk metric introduced by radion fluctuations, the radion itself was not calculated. Thus a scenario with a brane moving in the fixed bulk space-time was not excluded by the analysis of [7]. Such a scenario would be the natural analogue of the radion instability found in the two-dS brane model in [8]. In Section II B we will examine the case where the second brane is allowed to move in the fixed bulk metric, and solve the junction conditions giving its trajectory. We find that the second brane position is indeed unstable, with any displacement leading to the second brane going to infinity or colliding with the reference brane. However, it is shown that all brane quantities are completely regular at this collision. This is in contrast with the results of Webster and Davis [9], who examined similar non-BPS braneworld models with more general scalar field potentials, and found that the scalar field typically becomes divergent at a collision.

The stability of this scenario to homogenous metric perturbations is examined in a low-energy expansion in Section III. These results reinforce the stability found in [7]. We also demonstrate the ability of the low-energy expansion to reproduce a known exact solution in the correct limit.

**II. EXACT SOLUTION****A. Previous results**

The scalar field  $\Phi$  in the bulk has potential [5]:

$$\Lambda(\Phi) = \kappa^{-2} \left( \frac{\Delta}{8} + \delta \right) \sigma_0^2 e^{-2\sqrt{2}b\kappa\Phi(z,t)}, \quad (1)$$

and induced potentials on the two branes:

$$\lambda_{0,1}(\Phi) = \sqrt{2}\kappa^{-2}\sigma_{0,1}e^{-\sqrt{2}b\kappa\Phi(z,t)}, \quad (2)$$

where  $\Phi$  is taken to have a separable form:

$$\Phi(z, t) = \phi(t) + \Xi(z). \quad (3)$$

The parameter  $\Delta$  is defined in terms of the coupling constant  $b$  as

$$\Delta = 4b^2 - \frac{8}{3}. \quad (4)$$

Then the part of the bulk potential proportional to  $\Delta$  is the BPS potential, and tuned to the brane potentials such that the metric induced on the branes will be static (this is equivalent to the Randall-Sundrum tuning in the model with AdS bulk). The parameter  $\delta$  is a free parameter giving the deviation from this BPS tuning, and is what allows the time-dependent evolution on the brane.

The action for this model is given by

$$S = \int d^5x \sqrt{-g} \left[ \frac{1}{2\kappa^2} R - \frac{1}{2} \partial_\mu \Phi \partial^\mu \Phi - \Lambda(\Phi) \right] - \int d^4x \sqrt{-q_0} \lambda_0(\Phi) - \int d^4x \sqrt{-q_1} \lambda_1(\Phi). \quad (5)$$

Taking the bulk metric ansatz:

$$ds^2 = e^{2W(z)} [-dt^2 + e^{2\alpha(t)} d\vec{x}^2 + e^{2\sqrt{2}b\kappa\phi(t)} dz^2], \quad (6)$$

the Einstein equations are solved by [5]:

$$e^{\alpha(t)} = (H_0 t)^{2/(3\Delta+8)}, \quad (7)$$

$$e^{\sqrt{2}b\kappa\phi(t)} = H_0 t, \quad (8)$$

$$e^{W(z)} = \mathcal{H}(z)^{2/3(\Delta+2)}, \quad (9)$$

$$e^{\kappa\Xi(z)} = \mathcal{H}(z)^{2\sqrt{2}b/(\Delta+2)}, \quad (10)$$

with

$$H_0 = -\frac{3\Delta+8}{3(\Delta+2)}H, \quad H = -(\Delta+2)\sqrt{-\frac{\delta}{\Delta}}\sigma_0 \quad (11)$$

and for  $\Lambda < 0$ ,  $\mathcal{H}(z)$  is given by:

$$\mathcal{H}(z) = \sqrt{-1 - \frac{\Delta}{8\delta} \sinh Hz}. \quad (12)$$

We assume that  $-8/3 < \Delta < -2$  so that all exponents are finite, and that  $\Delta/8 + \delta < 0$  to ensure  $\Lambda < 0$ . Then we note that for  $\delta \neq 0$  a brane at position  $z = z_0$ , determined by  $\mathcal{H}(z_0) = 1$ , undergoes power-law inflation with scale factor  $a(t) = (H_0 t)^{2/(3\Delta+8)}$ ; and for a brane at this location bulk time  $t$  coincides with brane proper time.

A second brane may be introduced at arbitrary constant  $z = z_1$  as in [7]. Proper distance between the branes is then given by

$$L = H_0 t \int_{z_0}^{z_1} e^{W(z)} dz \propto t. \quad (13)$$

In the case of two dS branes the equilibrium position has constant proper distance; the time dependence of the power-law inflation on the brane causes a simple time dependence for the equilibrium proper distance. As  $H_0$  is positive, once the branes have emerged from the curvature singularity at  $t = 0$  they are always moving apart.

The junction conditions at the first brane are automatically satisfied; at the second brane they give a single equation relating  $z_1$  and the two brane tensions,  $\sigma_0$  and  $\sigma_1$ :

$$\sigma_1 = -2\sqrt{2}\sigma_0 \sqrt{-1 - \frac{\Delta}{8\delta} \sqrt{\frac{-\delta}{\Delta}} \cosh Hz_1}. \quad (14)$$

In proper time on the second brane the scale factor gives power-law inflation with the same exponent but a different constant of proportionality.

## B. Perturbing the equilibrium position

We now relax the assumption that the second brane has to be at constant  $z$  and perturb the brane from its equilibrium position found above. The governing equations are derived from the junction conditions and prove not to be analytically soluble, though a numeric solution can be obtained. Numeric solutions shown here have initial conditions close to, but slightly perturbed from the constant  $z$  brane position.

### 1. Junction conditions

The power-law inflation demonstrated in Section II A is induced by the action of the bulk scalar field on the brane, with the brane being empty apart from the scalar field potential (2). We now allow for matter with energy density  $\rho$  and pressure  $p$  on the second brane. Then we find the junction conditions and the scalar field matching conditions (given generally in [7]) at the second brane become:

$$[1 - (H_0 t \dot{z}_1)^2]^{-3/2} e^{-W} \left[ H_0 t \dot{z}_1 - H_0^3 t^2 \dot{z}_1^3 - W' H_0 t \dot{z}_1^2 + 2H_0 \dot{z}_1 + \frac{W'}{H_0 t} \right] = -\frac{\kappa^2}{6} \{ \lambda_1(\Phi) - 2\rho - 3p \}, \quad (15)$$

$$[1 - (H_0 t \dot{z}_1)^2]^{-1/2} e^{-W} \left[ \frac{W'}{H_0 t} + \frac{2H_0 \dot{z}_1}{3\Delta + 8} \right] = -\frac{\kappa^2}{6} \{ \lambda_1(\Phi) + \rho \}, \quad (16)$$

$$[1 - (H_0 t \dot{z}_1)^2]^{-1/2} e^{-W} \left[ \frac{W'}{H_0 t} + \frac{2H_0 \dot{z}_1}{3\Delta + 8} \right] = -\frac{\kappa^2}{6} \lambda_1(\Phi). \quad (17)$$

We can see that (16) and (17) are inconsistent unless  $\rho = 0$ . The bulk metric ansatz and the form of the scalar

field matching condition we have chosen do not allow for matter on the brane. It would be possible to add matter by taking a more general metric ansatz, or alternatively allowing a coupling of the scalar field to matter to change the form of Eq. (17) (as discussed in [10]). Here, however, we will investigate the case with no matter on the branes.

When  $\rho$  is taken to be zero, Eqs. (16) and (17) are equivalent, and Eq. (15) is equivalent to the derivative of these two.

To evaluate the effect of any deviation from the  $z_1 = \text{const}$  scenario previously considered we make the perturbation  $\bar{z}_1 \rightarrow \bar{z}_1 + \delta z$ , where  $\bar{z}_1$  is that value of  $z_1$  that satisfies Eq. (14) and  $\delta z$  is small. Then the linearized expansion of Eq. (16) gives:

$$\frac{1}{H_0 t} \delta(e^W W') + \frac{2H_0 e^{-W}}{3\Delta + 8} \delta z = \frac{2b}{6\kappa} \sigma_1 \frac{\Xi' e^{-\sqrt{2}b\kappa\Xi}}{H_0 t} \delta z. \quad (18)$$

When we substitute the solution for  $W$  and  $\Xi$  given (in the case  $\Lambda < 0$ ) by Eqs. (9)–(12), this simplifies to

$$-\frac{3(\Delta + 2)}{(3\Delta + 8)} \frac{\delta z}{t} = \delta \dot{z}. \quad (19)$$

This has solution  $\delta z \propto t^{-3(\Delta+2)/(3\Delta+8)}$ . For the range of  $\Delta$  we are considering, the exponent of  $t$  is positive, and hence the radion is unstable. We note that this solution agrees with the inverse Fourier transform of equation (49) of reference [7] in the case where all bulk metric perturbations are zero.

### 2. A numeric solution for the brane trajectory

To go beyond a linear analysis we solve Eq. (16) for  $\dot{z}_1$ :

$$\dot{z}_1 = \frac{72(3\Delta + 8)}{72H_0^2 \mathcal{H}^2 + \sigma_1^2 (3\Delta + 8)^2} \frac{\mathcal{H}}{t} \left[ -\frac{\mathcal{H}'}{3(\Delta + 2)} - \frac{\sqrt{2}}{12} \sigma_1 \sqrt{1 + \frac{\sigma_1^2 (3\Delta + 8)^2}{72H_0^2 \mathcal{H}^2} - \frac{(3\Delta + 8)^2}{9(\Delta + 2)^2} \frac{\mathcal{H}'^2}{H_0^2 \mathcal{H}^2}} \right]. \quad (20)$$

We introduce coordinates normalized with respect to reference brane tension  $\sigma_0$ :

$$H \rightarrow \frac{H}{\sigma_0}, \quad \sigma_1 \rightarrow \frac{\sigma_1}{\sigma_0}, \quad t \rightarrow \sigma_0 t, \quad z \rightarrow \sigma_0 z.$$

In order to obtain a numeric solution of the differential Eq. (20) we choose values for the parameters as:

$$\Delta = -\frac{9}{4}, \quad \delta = \frac{1}{4}, \quad H = \frac{1}{12}, \quad H_0 = \frac{5}{36}, \quad \sigma_1 = -2. \quad (21)$$

These have been chosen to be consistent with the definitions and inequalities presented in Section II A. Then the

position of the reference brane is given by

$$z_0 = 12 \sinh^{-1}(2\sqrt{2}) \approx 21.2, \quad (22)$$

and the tuned second brane position giving constant  $z_1$  is (from Eq. (14))

$$\bar{z}_1 = 12 \cosh^{-1}(6) \approx 29.7. \quad (23)$$

From Eqs. (12) and (20) we get the equation for  $z_1(t)$ :

$$\dot{z}_1 = \frac{36}{5} \frac{[\sinh(z_1/12) \cosh(z_1/12) - 6\sqrt{35}]}{[\cosh(z_1/12)]^2 + 35} t. \quad (24)$$

Figure 1 shows numeric solutions of this equation with initial conditions chosen so that the three curves show the trajectory of the second brane when it is initially at or slightly to either side of, the tuned position calculated above in Eq. (23). The reference brane position is also shown, and one can see that when the second brane is perturbed *towards* the reference brane, they will eventually collide.

### 3. Scale factor on the moving brane

As shown in [11] the five-dimensional Einstein equations can be projected onto a brane to obtain four-dimensional effective equations. In the case of a bulk scalar field with no matter on the branes, the effective four-

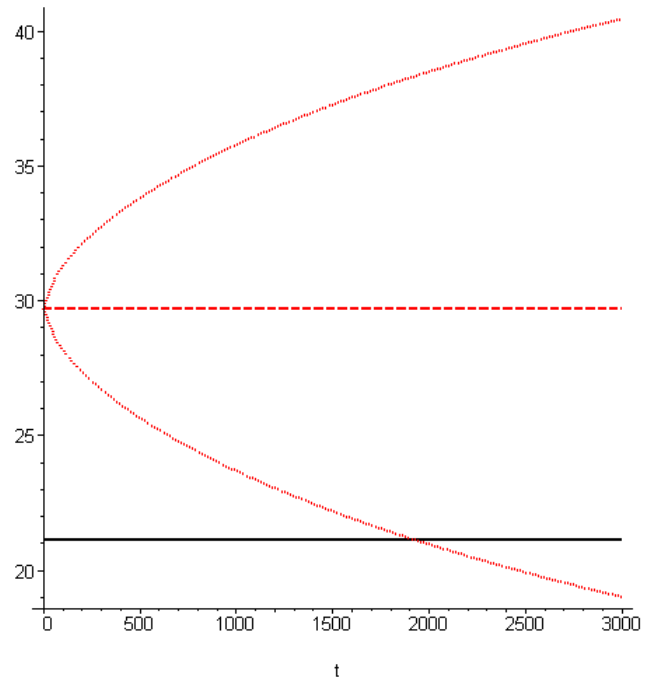


FIG. 1 (color online). Second brane position  $z_1(t)$  plotted against bulk coordinate time  $t$ . Initial conditions are  $z_1(0) = \bar{z}_1$  (dashed line) and  $z_1(0) = \bar{z}_1 \pm 0.1$  (dotted lines). The reference brane position is also shown (solid line). The solution for a brane perturbed towards the reference brane leads to a collision at time  $t_c \approx 1920$ , or brane proper time  $\tau_c \approx 919$ .

dimensional equations on the brane are [12]:

$${}^{(4)}G_{\mu\nu} = -\frac{\delta}{2}\sigma_0^2 e^{-2\sqrt{2}b\kappa\Phi} + \frac{2}{3}\kappa^2 T_{\mu\nu}(\Phi) - E_{\mu\nu}, \quad (25)$$

where  $T_{\mu\nu}(\Phi) = D_\mu\Phi D_\nu\Phi - \frac{5}{8}q_{\mu\nu}(D\Phi)^2$ , the covariant derivative on the brane is  $D_\mu$  and the induced metric on the brane is  $q_{\mu\nu}$ .  $E_{\mu\nu}$  is the projection of the bulk Weyl tensor onto the brane.

The Weyl part of these effective Einstein equations can be broken up into a piece dependent on  $\Phi$  and a piece independent of it as follows [13]:

$$\begin{aligned} -E_{\mu\nu} = & \sqrt{2}b\kappa[D_\mu\Phi D_\nu\Phi - q_{\mu\nu}D^2\Phi] \\ & + 2b^2\kappa^2[D_\mu\Phi D_\nu\Phi - q_{\mu\nu}(D\Phi)^2] \\ & + \frac{\kappa^2}{3}\left[D_\mu\Phi D_\nu\Phi - \frac{1}{4}q_{\mu\nu}(D\Phi)^2\right] \\ & + \frac{6b^2}{\Delta}\delta\sigma_0^2 e^{-2\sqrt{2}b\kappa\Phi}q_{\mu\nu} + F_{\mu\nu}. \end{aligned} \quad (26)$$

$E_{\mu\nu}$  is necessarily traceless, giving

$$F_\mu^\mu = 3\sqrt{2}b\kappa F_\Phi, \quad (27)$$

where  $3\sqrt{2}b\kappa F_\Phi$  is the trace of the  $\Phi$  part of  $E_{\mu\nu}$ , given by

$$F_\Phi = D^2\Phi + \sqrt{2}b\kappa(D\Phi)^2 - 4\sqrt{2}\frac{b\sigma_0^2\delta}{\kappa\Delta}e^{-2\sqrt{2}b\kappa\Phi}. \quad (28)$$

The bulk metric considered here is further constrained to have  $F_\Phi = 0 = F_{\mu\nu}$ , where  $F_\Phi = 0$  gives the wave equation for  $\phi$ .

The symmetries of the bulk metric combined with the wave equation for the scalar field determine the induced metric and scalar field on any brane in the bulk metric. There are insufficient degrees of freedom to allow for several independent solutions, with the result that these quantities will have the same  $\tau$ -dependence on a moving brane as on a fixed one. This result is demonstrated below using our numeric solution for the brane trajectory.

From the differential Eq. (24) and the form of the bulk metric we obtain the induced metric along the brane trajectory as:

$$ds_{(4)}^2 = -d\tau^2 + 256[\sinh(z_1/12)]^{-16/3}\left(\frac{5t}{36}\right)^{16/5}d\vec{x}^2, \quad (29)$$

where proper time  $\tau$  along the brane trajectory is related to bulk coordinate time  $t$  by

$$\frac{d\tau}{dt} = \frac{16}{[\sinh(z_1/12)]^{8/3}} \frac{6\cosh(z_1/12) + \sqrt{35}\sinh(z_1/12)}{[\cosh(z_1/12)]^2 + 35}. \quad (30)$$

Choosing the numeric solution for  $z_1$  with the second brane moving towards the reference brane, Eq. (30) can be solved numerically and inverted to get  $t(\tau)$ .

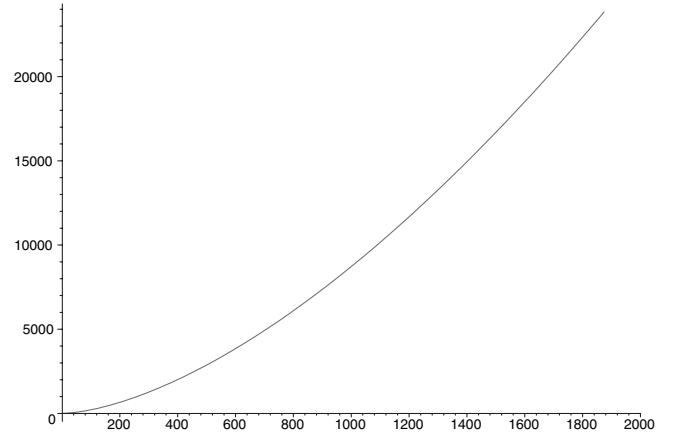


FIG. 2. Scale factor  $a_1$  on the second brane plotted against brane proper time  $\tau$  for the trajectory perturbed towards the reference brane. We can see that there is no singularity or other feature around the collision point  $\tau_c \approx 919$ .

From the induced metric (29) we have that the scale factor  $a_1$  on the second brane is

$$a_1 = \frac{16}{[\sinh(z_1/12)]^{8/3}} \left(\frac{5t}{36}\right)^{8/5}, \quad (31)$$

and, using (30), we have

$$H_1 = \frac{1}{a_1} \frac{da_1}{d\tau} = \frac{\sqrt{35}}{10t} [\sinh(z_1/12)]^{5/3}. \quad (32)$$

A plot of  $a_1(\tau)$  is shown in Fig. 2. A calculation of the quantity  $\tau H_1(\tau)$  in the numeric solution shows that it is constant at a value of  $2/(3\Delta + 8) = 8/5$ , demonstrating that the scale factor is power law with the same exponent as the nonmoving brane.

### C. Constraints on the bulk metric

In the above we have used a particular constrained form of the bulk metric whose symmetry properties discounting any possibility that the brane cosmology or the movement of the brane through the bulk affect the form of the bulk metric. In particular, the bulk scalar field and the bulk Weyl tensor are constrained to symmetric forms. This symmetry may be described in terms of the two quantities  $F_\phi$  and  $F_{\mu\nu}$  defined above.

Specifying the bulk metric ensures that this symmetry will not be disturbed if the brane is perturbed and starts to move. This results in a first order evolution equation for the radion, where other works have found second order equations [14]. Given an initial value for the radion, the brane velocity is fixed by the evolution equation. To set arbitrary initial position and velocity, we must allow for some perturbation of the bulk metric parameters.

Solving the full system of Einstein equations for a moving brane would be far too complicated to be practical, but if we use a low-energy expansion we can examine the

possibility for a more general bulk in the low-energy regime.

### III. LOW-ENERGY EXPANSION

The four-dimensional effective theory valid at low energies for a system with 2 branes is derived in [15,16] and applied to a bulk scalar field in [17]. We will substitute the potentials from Eqs. (1) and (2) into this low-energy formalism to determine the validity of allowing free brane motion while constraining the bulk to the static metric given in [5].

In this low-energy theory, there are essentially three moduli fields  $\hat{\alpha}$ ,  $\hat{\phi}$ , and  $d$ .  $\hat{\alpha}$  and  $\hat{\phi}$  correspond to the scale factor and the scalar field on the reference brane, and  $d$  encodes an arbitrary variation of the proper distance between the branes; the proper distance being given by the formula

$$L = e^{\sqrt{2}b\hat{\phi}} d(t). \quad (33)$$

In this section we will use the variables and parameters of [17], but to ensure we are describing the physical system set up previously, the parameters must be given by  $\sigma = \sigma_0$ ,  $V(\phi) = -2\delta\sigma^2 e^{-2\sqrt{2}b\phi}$ ,  $U(\phi) = 0$ , and  $\tilde{U}(\phi) = \sigma'\sqrt{2}/\kappa^2 e^{-\sqrt{2}b\phi}$ , where  $\sigma' = \sigma_0 - \sigma_1$ ; then the action given in [17] reduces to that of Eq. (5).

The low-energy expansion given in [17] relies on the assumption

$$\sigma \gg \kappa^2 \rho, \kappa^2 p, \sigma^{-1} V, \kappa^2 U, \kappa^2 \tilde{U}, \quad (34)$$

which in our case implies

$$\delta \ll 1, \quad \sigma' \ll \sigma. \quad (35)$$

In the  $d = d_*$  = constant,  $z_1 = \text{constant}$  case we can derive the coordinate transformation between the exact metric given by Eqs. (7)–(10) and the approximate one of [17] as:  $x \rightarrow x$ ,  $t \rightarrow t$ , and

$$y \rightarrow \frac{12}{\sqrt{2}(3\Delta + 8)d_*\sigma} \times \left[ 1 - \left( \sqrt{-1 - \frac{\Delta}{8\delta} \sinh(Hz)} \right)^{(3\Delta+8)/[3(\Delta+2)]} \right] \quad (36)$$

(valid at low energies and small  $\delta$  only). From this transformation and the low-energy conditions (35), we can derive the condition on the exact solution that  $H z < H z_1 \ll 1$ . We suppose that this condition would also hold when  $d$  is not constant.

#### A. Linear approximation

The effective equations on the brane are given by equations (58)–(60) in [17]. To evaluate the effect of some small deviation from the  $z_1 = \text{constant}$ ,  $d = \text{constant}$  scenario we make a linear perturbation  $d = d_* + \delta_d$  where  $\delta_d$  is small compared to  $d_*$ . We assume that  $\sigma'$  is the tuned

brane tension to keep  $d$  at constant  $d_*$ :

$$\sigma' = \frac{4\delta\sigma}{\Delta} [(1 - d_*)^{(6\Delta+12)/(3\Delta+8)} - 1] \quad (37)$$

and that any deviation of  $\hat{\phi}$  and  $\hat{\alpha}$  from their values in the exact solution is also of order  $\delta_d$  or smaller. Under these assumptions, the evolution equation for  $d$  decouples from the governing equations for  $\hat{\phi}$  and  $\hat{\alpha}$ , and gives a second order ordinary differential equation,

$$\ddot{\delta}_d + \left( \frac{3\Delta + 14}{3\Delta + 8} \right) \frac{\dot{\delta}_d}{t} - \left[ \frac{9\Delta(\Delta + 2)}{(3\Delta + 8)^2} \right] \frac{\delta_d}{t^2} = 0. \quad (38)$$

Substituting  $F_\phi = 0$  into the evolution equation for  $\phi$  obtained in the low-energy expansion and combining with the radion evolution Eq. (38) gives a first order equation

$$\dot{\delta}_d = - \frac{3(\Delta + 2)}{(3\Delta + 8)} \frac{\delta_d}{t}. \quad (39)$$

The second order evolution Eq. (38) has two independent solutions:

$$\delta_d \propto t^{-3(\Delta+2)/(3\Delta+8)}, \quad (40)$$

$$\delta_d \propto t^{3\Delta/(3\Delta+8)}. \quad (41)$$

The growing mode (40) satisfies the  $F_\phi = 0$  condition (39), while the decaying mode (41) does not. If one chooses initial conditions for the brane motion satisfying  $F_\phi = 0$ , they specify solely the growing mode, so a solution that starts with  $F_\phi = 0$  will remain that way for all time. The one-parameter family of solutions Section II B must lie along this growing-mode trajectory. Any solution that also contains some decaying mode solution will not have  $F_\phi = 0$ , but it will tend towards a trajectory that does, implying that  $F_\phi = 0$  is in some sense an attractor.

To demonstrate more clearly the nature of the solutions to the linearized evolution equation for  $d$ , we present a phase-plane analysis. To transform Eq. (38) to an autonomous form, we make a change of variable to  $s = \frac{2}{(3\Delta+8)} \ln t$ . Using this new time coordinate, the evolution equation becomes

$$\delta_d'' + 3\delta_d' - \frac{9}{4}\Delta(\Delta + 2)\delta_d = 0, \quad (42)$$

where a prime denotes the derivative with respect to  $s$ . If we put  $X = \delta_d$  and  $Y = \delta_d'$ , then the system can be written

$$X' = Y, \quad Y' = \frac{9}{4}\Delta(\Delta + 2)X - 3Y. \quad (43)$$

The system has only one equilibrium point, at  $X = Y = 0$ . The eigenvalues of the system around this point are  $\frac{3\Delta}{2}$  and  $\frac{-3(\Delta+2)}{2}$ , with the first negative and the second positive. Thus  $X = Y = 0$  is a saddle point. The equilibrium lines of this saddle point are found to be  $Y = \frac{3\Delta}{2}X$  and  $Y = \frac{-3(\Delta+2)}{2}X$ . The Eqs. (43) show that the phase trajectories

go from left to right, i.e. towards the equilibrium line with positive gradient. Converting the equilibrium lines back to our original coordinates confirms that they correspond to the solutions (40) and (41), respectively, and that the growing mode (40) is an attractor line. The phase diagram for  $\Delta = -\frac{9}{4}$  is shown in Fig. 3.

Earlier we made the assumption that  $\hat{\alpha}$  and  $\hat{\phi}$  differed only by a small amount from the background solution. We now quantify this as

$$\hat{\alpha} = \frac{2 \ln(H_0 t)}{(3\Delta + 8)} + \delta_\alpha(t), \quad \hat{\phi} = \frac{\ln(H_0 t)}{\sqrt{2}b} + \delta_\phi(t), \quad (44)$$

where  $\delta_\alpha$  and  $\delta_\phi$  are small relative to the background. Now the linear reduction of the remaining evolution equations from [17] is obtained as:

$$\begin{aligned} \ddot{\delta}_\phi + \frac{3}{\sqrt{2}b} \frac{\dot{\delta}_\alpha}{t} + \frac{(6\Delta + 22)}{(3\Delta + 8)} \frac{\dot{\delta}_\phi}{t} + \frac{12}{(3\Delta + 8)} \frac{\delta_\phi}{t^2} \\ = \frac{-18\sqrt{2}b(\Delta + 4)}{(3\Delta + 8)^2} \xi(d_*) \left[ \frac{\dot{\delta}_d}{t} + \frac{3(\Delta + 2)}{(3\Delta + 8)} \frac{\delta_d}{t^2} \right], \end{aligned} \quad (45)$$

$$\ddot{\delta}_\alpha + \frac{8}{(3\Delta + 8)} \frac{\dot{\delta}_\alpha}{t} + \frac{1}{3\sqrt{2}bt} \frac{\dot{\delta}_\phi}{t} - \frac{6\Delta\sqrt{2}b}{(3\Delta + 8)^2} \frac{\delta_\phi}{t^2} = 0, \quad (46)$$

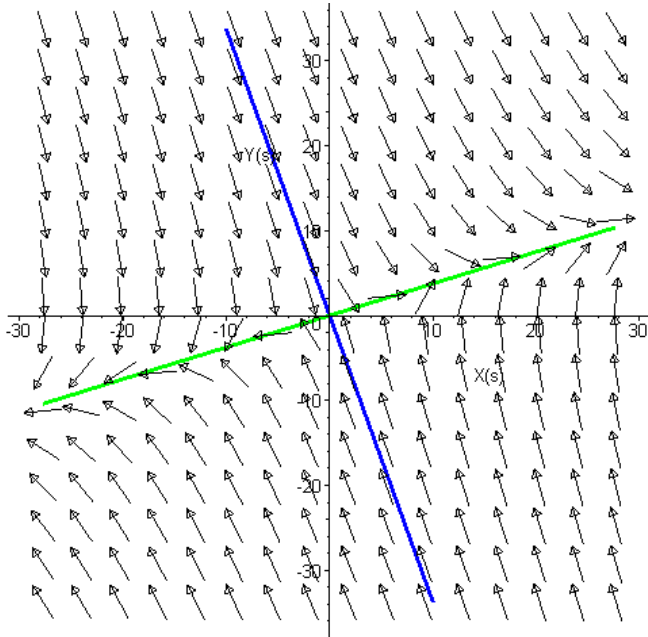


FIG. 3 (color online). Phase plane for the linearized evolution of  $d$  when  $\Delta = -\frac{9}{4}$ . The line with positive gradient corresponds to the growing mode for  $d$  shown in Eq. (40), and the line with negative gradient corresponds to the decaying mode (Eq. (41)).

$$\frac{\dot{\delta}_\alpha}{t} + \frac{2\sqrt{2}b}{(3\Delta + 8)} \frac{\delta_\phi}{t^2} = \frac{-2}{(3\Delta + 8)} \xi(d_*) \left[ \frac{\dot{\delta}_d}{t} + \frac{3(\Delta + 2)}{(3\Delta + 8)} \frac{\delta_d}{t^2} \right], \quad (47)$$

where

$$\xi(d_*) = \frac{(1 - d_*)^{4/(3\Delta+8)}}{\{1 - (1 - d_*)^{(3\Delta+12)/(3\Delta+8)}\}}.$$

The system (38) and (45)–(47) has a general solution of the form

$$\delta_d = d_1 t^{-3(\Delta+2)/(3\Delta+8)} + d_2 t^{3\Delta/(3\Delta+8)}, \quad (48)$$

$$\begin{aligned} \delta_\phi = \phi_1 t^{-1} + \phi_2 t^{-6/(3\Delta+8)} - d_2 \xi(d_*) \\ \times \frac{3(\Delta + 1)}{\sqrt{2}b(3\Delta + 4)} t^{3\Delta/(3\Delta+8)}, \end{aligned} \quad (49)$$

$$\begin{aligned} \delta_\alpha = \frac{2\sqrt{2}b}{(3\Delta + 8)} \left[ \phi_1 t^{-1} + \frac{(3\Delta + 8)}{6} \phi_2 t^{-6/(3\Delta+8)} \right] \\ - d_2 \xi(d_*) \frac{6(\Delta + 1)}{(3\Delta + 8)(3\Delta + 4)} t^{3\Delta/(3\Delta+8)} + c_\alpha, \end{aligned} \quad (50)$$

where  $d_1, d_2, \phi_1, \phi_2,$  and  $c_\alpha$  are all arbitrary constants of integration. However, we can neglect  $c_\alpha$  as it is a gauge mode corresponding to a redefinition of the ordinary spatial coordinates. We can then see from the form of this solution that any perturbation to the background metric functions  $\hat{\alpha}, \hat{\phi}$  will decay (in the linear regime at least).

## B. Full nonlinear low-energy evolution

Having completed the linear analysis, we solve the full nonlinear system of low-energy equations numerically, to see if the results above are substantially changed in the nonlinear regime. The parameters chosen for this numerical analysis are

$$\Delta = -\frac{9}{4}, \quad \delta = \frac{1}{100}, \quad H = \frac{1}{60}, \quad H_0 = \frac{1}{36}, \quad (51)$$

(the value of  $\delta$  chosen for the previous numerical simulation was too large to be valid in the low-energy approximations, so more appropriate values have been chosen). The background value of  $d$  is taken to be  $d_* = 0.5$  and the corresponding tuned value of the potential on the second brane is  $\sigma' \simeq -0.023$ . Figure 4 shows the numerical analysis (dotted curves) compared to the solution for the radion evolution from the linear regime, shown as the solid curve. We can see that at early time our linear approximation is reasonably accurate, but that as the collision is approached the two curves are widely divergent.

The dotted curves show the results for the numerical simulation with two different sets of initial conditions—



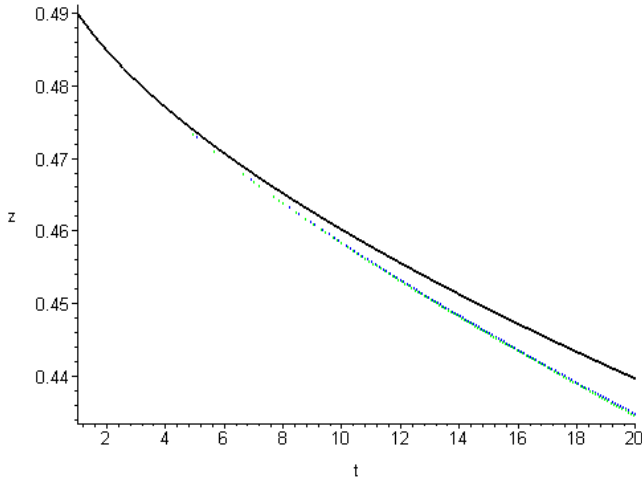


FIG. 4 (color online). Numerical simulations of the nonlinear radion evolution (dotted lines) are compared to the solution for the radion in the linear regime (solid line).

one set of initial conditions corresponds to the growing mode identified in the linear analysis, and hence to the brane trajectories identified in the exact solution, whereas the other set corresponds to a mixture of the growing and decaying modes. The numerical solution for  $\hat{\alpha}$  and  $\hat{\phi}$  under these initial conditions shows that while they have identically the form of the background solution for the growing-mode conditions, the mixed-mode initial conditions set an initial perturbation away from the background solution which quickly decays to 0 (or to the constant gauge mode in the case of  $\hat{\alpha}$ ). This confirms the stability of the background solution to perturbations of the brane position that was demonstrated in the linear regime.

**C. Accuracy of the low-energy approximation and simulations**

Figures 5 and 6 show the proper distance between the two branes (given in Eq. (33)) as obtained from the numerical integration of the low-energy effective equations and from the numerical solution for the brane trajectory in the exact bulk metric solution, plotted for several different values of the parameter  $\delta$ . There is some difference between the exact and low-energy curves, but we can see this difference decreasing as  $\delta$  decreases, indicating that the integration of the low-energy equations is accurate in the limit  $\delta \rightarrow 0$ . Figure 5 demonstrates the sensitivity of the system to even small changes in  $\delta$ , whereas Fig. 6 demonstrates the wide deviation of the approximate solution from the exact solution when  $\delta$  becomes larger.

Figure 7 demonstrates the sensitivity of both solutions to a change in initial conditions. An increase in the initial perturbation in the distance between the branes dramatically decreases the time to the brane collision.

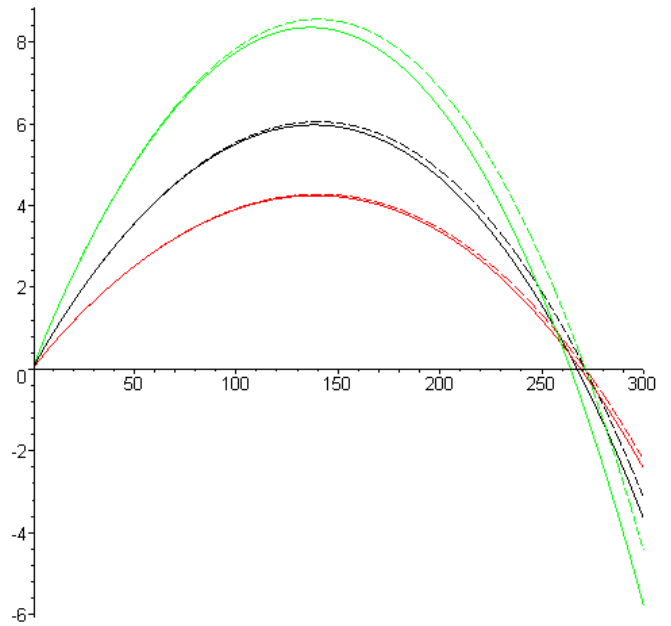


FIG. 5 (color online). The proper distance between the two branes as given by the exact solution (solid lines) and low-energy nonlinear equations (dashed lines), plotted for  $\delta = 1/200$  (lowest),  $\delta = 1/100$  (middle), and  $\delta = 1/50$  (highest).

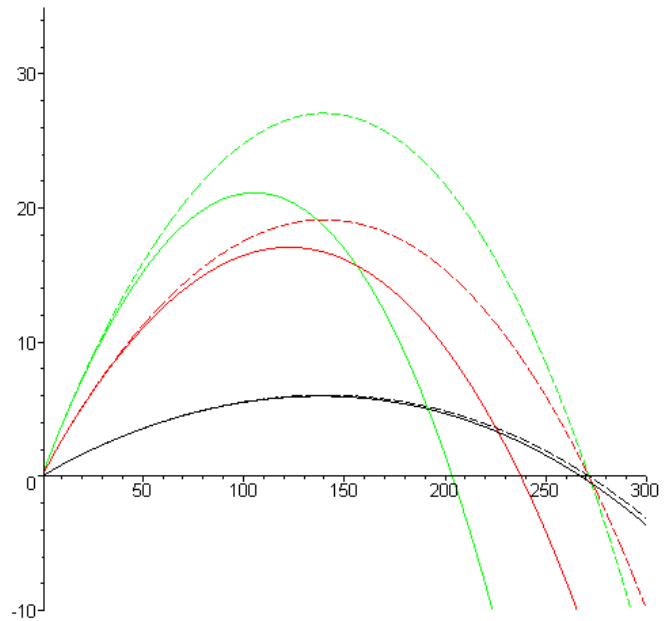


FIG. 6 (color online). The proper distance between the two branes as given by the exact solution (solid lines) and low-energy nonlinear equations (dashed lines), plotted for  $\delta = 1/5$  (highest),  $\delta = 1/10$  (middle), and  $\delta = 1/100$  (lowest).

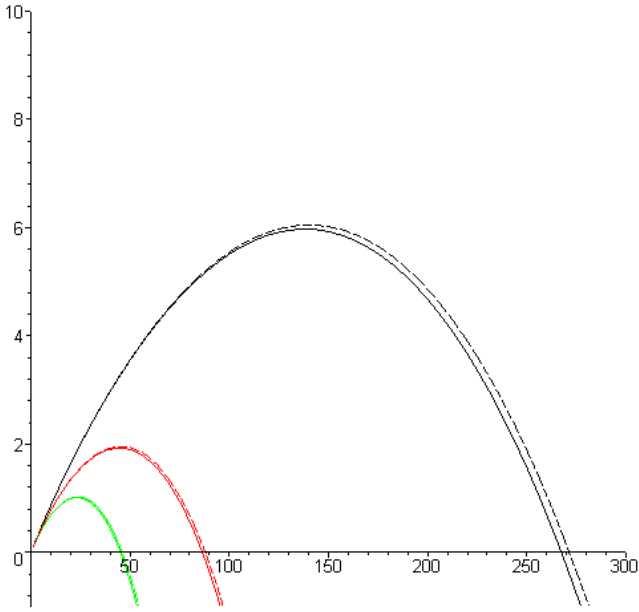


FIG. 7 (color online). The proper distance between the two branes as given by the exact solution (solid lines) and low-energy nonlinear equations (dashed lines), plotted for a variety of initial perturbations of  $d$  ( $\delta_d = 0.01, 0.02, 0.03$ ). Time to the collision decreases with increasing initial perturbation.

#### IV. CONCLUSIONS

In this paper we have demonstrated that for the bulk metric with scalar field given in [5] there is an instability in the position of a second brane. Solving for the trajectory of this second brane shows that the instability can lead to a collision between the two branes. The scale factor and scalar field are shown to retain the same dependence on brane proper time regardless of the motion of the brane, and hence remain regular at the collision. It was found in [9,18] that a general class of potentials for 2-brane systems with bulk scalar field will result in a singularity at any collision; however it was found in [18], as here, that the exponential potential is exceptional and can tame the singularities at the collision.

It is also worth noting that (for a countably infinite subset of the possible values of the parameters  $b$  and  $\Delta$ )

the scalar field potential used here can be reproduced from a compactification of an empty higher-dimensional space [19,20], with the dimensionality determining the values of  $\Delta$  and  $b$ . In this picture the collision is singular in that the bulk space-time loses a dimension when the space between the brane disappears, however the induced metric of the brane and compactified space remains regular, and hence the effective scalar field derived from the compactified volume will remain regular also.

In a complementary approach we considered the system using a low-energy expansion developed in [17]. This expansion reproduces the solution found in the previous section to good accuracy in the correct limit (see Fig. 5). The low-energy equations also identify a solution excluded by the methods used previously, in which the initial perturbation of the second brane necessitates a perturbation of the bulk metric away from its background. This solution quickly decays toward the original solution with the unperturbed bulk, confirming the conclusion of [7] that there can be no unstable homogeneous perturbations of the bulk metric.

It would be interesting to see if the capability of solving the cosmological perturbations demonstrated in Koyama and Takahashi's one-brane solution [6] is reproduced in this two-brane model. The perturbations would diverge as the branes approach collision, but it is possible to match divergent perturbations across a collision in some scenarios (see e.g. [21]). If this is possible it would give an interesting parallel to the ‘‘Born-again braneworld’’ [21], the cyclic model [22], and other pre-big-bang scenarios. A microscopic particle-theoretic understanding of interactions at the collision would be helpful in determining the dynamics at the collision (whether the branes are likely to pass through each other as in [21,22], coalesce as in [23,24], or disintegrate as in [25]), as well as the behavior of perturbations near the collision. However there are techniques available to evolve perturbations through brane collisions at a purely classical level [21,26].

#### ACKNOWLEDGMENTS

E. L. is supported by EPSRC; K. K. and R. M. are supported by PPARC.

- 
- [1] L. Randall and R. Sundrum, Phys. Rev. Lett. **83**, 3370 (1999); L. Randall and R. Sundrum, Phys. Rev. Lett. **83**, 4690 (1999).
  - [2] R. Maartens, D. Wands, B. A. Bassett, and I. Heard, Phys. Rev. D **62**, 041301 (2000).
  - [3] Y. Himemoto and M. Sasaki, Phys. Rev. D **63**, 044015 (2001).
  - [4] S. Kobayashi, K. Koyama, and J. Soda, Phys. Lett. B **501**, 157 (2001).
  - [5] K. Koyama and K. Takahashi, Phys. Rev. D **67**, 103503 (2003).
  - [6] K. Koyama and K. Takahashi, Phys. Rev. D **68**, 103512 (2003).
  - [7] S. Mukohyama and A. Coley, Phys. Rev. D **69**, 064029 (2004).
  - [8] U. Gen and M. Sasaki, Prog. Theor. Phys. **105**, 591 (2001).



- [9] S. L. Webster and A. C. Davis, hep-th/0410042.
- [10] D. Langlois and M. Rodriguez-Martinez, Phys. Rev. D **64**, 123507 (2001).
- [11] T. Shiromizu, K. I. Maeda, and M. Sasaki, Phys. Rev. D **62**, 024012 (2000).
- [12] K. I. Maeda and D. Wands, Phys. Rev. D **62**, 124009 (2000).
- [13] H. Yoshiguchi and K. Koyama, Phys. Rev. D **70**, 043513 (2004).
- [14] P. Binetruy, C. Deffayet, and D. Langlois, Nucl. Phys. **B615**, 219 (2001); I. R. Vernon and A. C. Davis, hep-ph/0401201.
- [15] S. Kanno and J. Soda, Phys. Rev. D **66**, 043526 (2002).
- [16] T. Shiromizu and K. Koyama, Phys. Rev. D **67**, 084022 (2003).
- [17] S. Kobayashi and K. Koyama, J. High Energy Phys. **12** (2002) 056.
- [18] J. Martin, G. N. Felder, A. V. Frolov, M. Peloso, and L. A. Kofman, Phys. Rev. D **69**, 084017 (2004).
- [19] M. Cvetič, H. Lü, and C. N. Pope, Phys. Rev. D **63**, 086004 (2001).
- [20] T. Kobayashi and T. Tanaka, Phys. Rev. D **69**, 064037 (2004).
- [21] S. Kanno, M. Sasaki, and J. Soda, Prog. Theor. Phys. **109**, 357 (2003).
- [22] See e.g. P. J. Steinhardt and N. Turok, Phys. Rev. D **65**, 126003 (2002).
- [23] S. Kanno, J. Soda, and D. Wands, J. Cosmol. Astropart. Phys. **08** (2005) 002.
- [24] S. A. Abel and J. Gray, J. High Energy Phys. **11** (2005) 018.
- [25] W. Chen, Z. W. Chong, G. W. Gibbons, H. Lü, and C. N. Pope, Nucl. Phys. **B732**, 118 (2006).
- [26] A. J. Tolley, N. Turok, and P. J. Steinhardt, Phys. Rev. D **69**, 106005 (2004).